Journal of Magnetism and Magnetic Materials 380 (2015) 13–19

Contents lists available at ScienceDirect

Journal of Magnetism and Magnetic Materials

journal homepage: www.elsevier.com/locate/jmmm

In vitro cytotoxicity of Fe–Cr–Nb–B magnetic nanoparticles under high frequency electromagnetic field

Horia Chiriac [a,*], Tudor Petreus [b], Eugen Carasevici [b], Luminita Labusca [a], Dumitru-Daniel Herea [a], Camelia Danceanu [a], Nicoleta Lupu [a]

[a] *National Institute of Research and Development for Technical Physics, Iasi, Romania*
[b] *"Gr.T. Popa" University of Medicine and Pharmacy, Iasi, Romania*

ARTICLE INFO

Article history:
Received 30 June 2014
Received in revised form
3 October 2014
Accepted 4 October 2014
Available online 13 October 2014

Keywords:
Magnetic hyperthermia
Magnetic nanoparticles
Biocompatibility
Curie temperature

ABSTRACT

The heating potential, cytotoxicity, and efficiency of $Fe_{68.2}Cr_{11.5}Nb_{0.3}B_{20}$ magnetic nanoparticles (MNPs), as such or coated with a chitosan layer, to decrease the cell viability in a cancer cell culture model by using high frequency alternating magnetic fields (AMF) have been studied. The specific absorption rate varied from 215 W/g for chitosan-free MNPs to about 190 W/g for chitosan-coated ones, and an equilibrium temperature of 46 °C was reached when chitosan-coated MNPs were subjected to AMF. The chitosan-free $Fe_{68.2}Cr_{11.5}Nb_{0.3}B_{20}$ MNPs proved a good biocompatibility and low cytotoxicity in all testing conditions, while the chitosan-coated ones induced strong tumoricidal effects when a cell–particle simultaneous co-incubation approach was used. In high frequency AMF, the particle-mediated heat treatment has proved to be a critical cause for decreasing *in vitro* the viability of a cancer cell line.

1. Introduction

The incidence of cancerous disease is expected to increase worldwide by more than 75% by the year 2030 [1]. Consequently, one of the most important challenges in biomedical research is focusing on finding novel efficient therapies or reducing the side effects of the current treatments. Apart from the conventional medical methods based on chemotherapy and radiotherapy, different heating-based approaches are considered increasingly. The thermotherapy making use of the latest materials and technological advances represents a reliable solution for treatment, as the cancer cells are reported to be more heat-vulnerable than normal ones. The cancer cells should withstand a temperature increase of 41–47 °C to initiate irreversible intra- or extra-cellular degradation mechanisms capable to induce necrotic processes within tumors. A heating process that does not elevate the temperature of the biological tissue above 45–47 °C can be carried out through magnetic hyperthermia.

The majority of reported studies focusing on magnetic hyperthermia have generally made use of magnetite (Fe_3O_4) and related spinels with cobalt, nickel, or other substitutions, ranging from several nanometers to tens of microns [2,3]. However, the heating of Fe-oxides (mainly Fe_3O_4) up to moderate temperatures (below 47 °C), and, most importantly, the capacity to retain the temperature in the range of 41–46 °C require a very rigorous control of the power of the high frequency generator. To address this issue, we have developed a new type of ferromagnetic nanoparticles (MNPs) based on glassy Fe–Cr–Nb–B alloys with Curie temperature that can be adjusted relatively easily and precisely in the 30–50 °C interval by tuning the Cr content, in order to be more suitable for self-regulating magnetic hyperthermia [4,5]. The purpose of this work was to quantify the cytotoxicity of Fe–Cr–Nb–B MNPs, without or with a supplementary coating chitosan layer, and to evaluate the MNPs efficiency to decrease the cell viability in a cell culture model by using high frequency A.C. magnetic fields (AMF). Also, the heating efficiency in terms of caloric output and equilibrium temperature was studied. The very good biochemical features such as biocompatibility, biodegradability, film forming ability, gelation characteristics, bioadhesion [6] and antitumoral properties [7] of chitosan are well known. Because of its versatility, chitosan was used extensively to coat metallic nanoparticles, including the ones used for hyperthermia applications [6,8], immobilization of enzymes on electrodes in electrochemical biosensors [9], drug delivery for administration of either biomacromolecules or low molecular weight drugs [10], etc. Chitosan is also considered an almost ideal biomaterial for cell culture applications, whereas the cell cultures model represent the most practical approach to evaluate biocompatibility and biotoxicity [11].

* Corresponding author.
E-mail address: hchiriac@phys-iasi.ro (H. Chiriac).

http://dx.doi.org/10.1016/j.jmmm.2014.10.015
0304-8853/

2. Experimental

2.1. Experimental setup

The heating power of magnetic nanoparticles and the heating influence on the cell viability were investigated by using a magnetic-induction hyperthermia unit. The heating setup consists of the radio frequency power supply and heating station (Hüttinger TIG 10/300), the coil (home-made) and the chiller (water as refrigerant). For experiments, in order to minimize the heat exchange with the environment, the samples were placed inside a double layered glass vessel, with medium-to-low vacuum between the double layers, surrounded by a polystyrene box (Fig. 1). The samples were placed in the center of the inductive coil and a fixed current was employed to generate an alternating magnetic field at a frequency of 153 kHz. A magnetic induction of 350 mT was measured in the center of the solenoid.

2.2. Preparation of Fe–Cr–Nb–B magnetic nanoparticles

The details about the preparation of Fe–Cr–Nb–B MNPs are described elsewhere [5]. Briefly, a rapidly quenched $Fe_{68.2}Cr_{11.5}Nb_{0.3}B_{20}$ amorphous ribbon was milled in a planetary ball mill (PM-200 Retsch) operating at 550 rpm, in oleic acid. We used oleic acid to avoid the oxidation of the MNPs during the milling, and not for coating purposes. After milling, the obtained metallic nanopowders, labeled as sample C (uncoated or chitosan-free MNPs), with sizes of 20–40 nm, were stored under nitrogen atmosphere for subsequent characterization and testing.

2.3. Preparation of chitosan-coated MNPs

Prior to coating with polymer, MNPs have been washed with 10% (w/v) NaOH solution, under ultrasonication, in order to remove the remaining oleic acid from the surface of the milled MNPs. Two chitosan-coated samples, labeled as A and B, have been prepared. The coating approach employed the precipitation of chitosan in an alkaline solution. The chitosan was dissolved in 5 ml solution of 4% (v/v) acetic acid, under ultrasonication (US). 140 mg of Fe–Cr–Nb–B MNPs were added over chitosan solution and the whole mixture was ultrasonicated for 1 min. Then, the magnetic suspension was transferred into 50 ml solution of acetic acid 4%, followed by the addition of 50 ml solution of NaOH (10%), under ultrasonication and mechanic agitation (700 rpm). After dropping 10 ml ethylic alcohol into chitosan-MNPs suspension, the magnetic composite was magnetically separated and washed with distilled water until a neutral pH was reached.

Fig. 2 presents the infrared spectra of the chitosan-free and chitosan-coated magnetic nanoparticles. The chitosan-coated MNPs show a more complex IR spectrum compared with the one of chitosan. However, the chitosan-coated MNPs show specific absorption peaks at 3440 cm^{-1}, corresponding to $\bar{NH_2}$ and $\bar{OH}$ groups [12]. The peaks at 2920 $cm^{-1}$and 2875 cm^{-1} correspond to the streching of C–H bond in $\bar{CH_2}$ and $\bar{CH_3}$, respectively [13], whilst the one at 1598 cm^{-1} can be assigned to C=O stretching vibration [14]. At 1096 cm^{-1} appears the peak for C–O stretching of primary alcoholic group [6] and at 1030 cm^{-1} the one for the primary hydroxyl group (the characteristic peak of CH_2-OH in primary alcohols, C–O stretch) in chitosan [12].

5 mg of chitosan have been used for sample A, which has a weight ratio chitosan/MNP of ~3.5%, while 14 mg of chitosan have been used for sample B with the final weight ratio chitosan/MNP of ~10%. TG measurements (Fig. 3), carried out in argon atmosphere using a NETZSCH STA 409 PC/PG, at a heating rate of 2 K/min., confirmed that the weight ratio of chitosan/MNPs is close to 3.5% and 10%, respectively. The weight decrease of about 0.1% for sample C (chitosan-free MNPs), ~1.4% for sample A and ~4.1% for sample B, respectively, below 160 °C is caused by the loss of the water of hydration from the investigated MNPs. The next decrease of 3.4% for sample A and 9.6% for sample B is attributed to the decomposition of the chitosan.

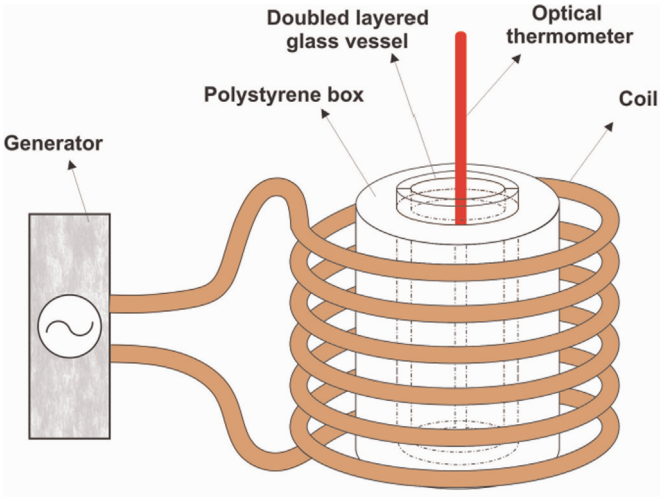

Fig. 1. Experimental setup for calorimetric measurements.

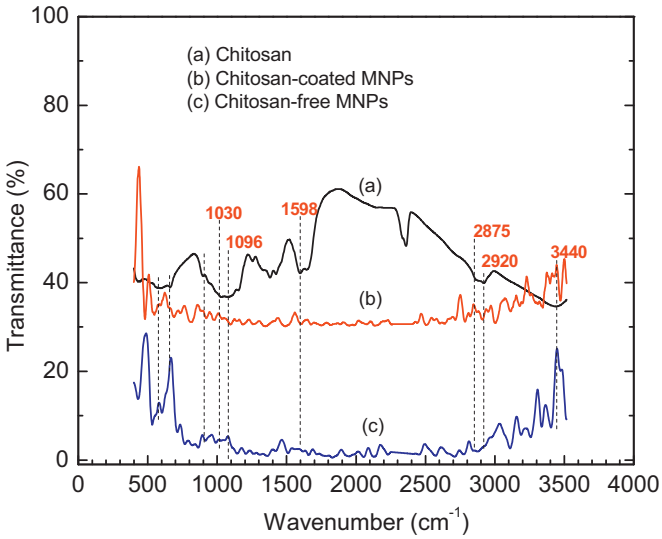

Fig. 2. FTIR spectra of (a) chitosan, (b) chitosan-coated MNPs (sample A), (c) chitosan-free MNPs.

2.4. MNPs conditioning

MNPs were sterilized for 30 min. using an UV-transilluminator, followed by the dispersion of chitosan-coated and chitosan-free MNPs, respectively, in sterile phosphate buffered saline solution at a concentration of 10 mg nanoparticles/ml (MNPs stock suspensions). The concentration was calculated with respect to the uncoated (chitosan-free) MNPs.

2.5. Cell culture preparation

For "*in vitro*" experiments, the human osteosarcoma cell line (Eppelheim, Germany) was used. Osteosarcoma cell line was chosen based on the previous experience in their relatively rapid expansion rate that allow obtaining high amount of cell population required for different tests. The cells thawing was done by immersion in a thermostated water bath (37 °C), than the cells

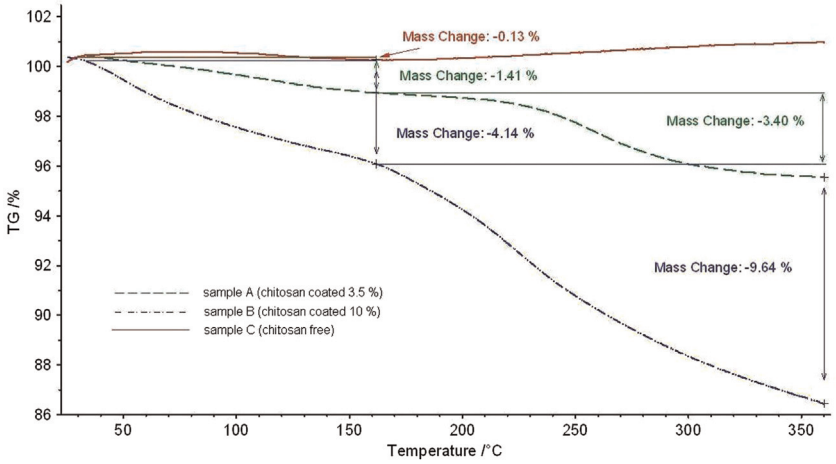

Fig. 3. TG measurements of samples A and B (chitosan-coated MNPs) and sample C (chitosan-free MNPs).

were washed with complete culture medium-MEM (Minimal Eagle Medium) supplemented with 10% fetal bovin serum, 2% L-glutamine and 1% antibiotic (penicillin–streptomycin). After centrifugation at 300 g, the cells were re-suspended in 10 ml complete medium, and subcultivated in 25 cm^2 flasks. After 48 h, the cells were detached from the flask using trypsin–EDTA solution. Following the addition of complete medium, the suspension was centrifugated at 300 g for 5 min., and the resulted pellets were re-suspended in 1 ml complete medium. The cell density was determined by using a Neubauer cell counting chamber. Finally, the cells were seeded into 4 flasks (75 cm^2) and incubated at 37 °C, 5% CO_2, and 95% humidity.

2.6. Cytotoxicity evaluation

In all the cytotoxicity experiments cells lines were used at 85–90% confluence, within the logarithmic growth phase. As tumor cell lines have a relatively high growth rate, confluence was achieved 48 h after thawing and similar is true for the subculture period.

For MNPs cytotoxicity evaluation, three situations were considered:

- *Simultaneous co-incubation* of the cells with magnetic nanoparticles, which assumed the transfer of previously subcultivated cells into a 96-well plate (density of 5×10^4 cells/well) followed by the addition of MNPs 2–3 min. later and co-incubation for 12 h.
- *Incubation of cells first* (same density as in the first case), followed by 6 h-delayed addition of MNPs and incubation for 12 h.

For both cases, 4 concentrations of MNPs were used (Table 1). The volume of the samples was imposed by the optimum capacity of the plates' well, whereas the concentration was arbitrarily established.

- *Cytotoxicity in AC magnetic fields*. The experiments carried out in AC magnetic fields were essentially based on the procedure described above for AMF-free toxicity tests. Briefly, the cancer cells were cultivated in 6 flasks that reached 90% confluence after 72 h of incubation. For tests, 2.5 ml from the obtained cell suspension were equally distributed in 5 sterile polypropylene tubes at a density of 10^6 cells/ml. Next, 2.5 ml from the MNPs stock suspension (10 mg/ml) were equally added in the tubes. One MNPs-free tube, containing 1 ml cell suspension, was used as control. The samples, previously incubated at 37 °C in a water bath, were placed one by one in the center of the coil and submitted to AMF heating for 20 min. Other 6 control samples were simultaneously incubated in a thermostated water bath, in AMF-free conditions, at 37 °C for 20 min. Following the AMF heating, the magnetic nanoparticles were settled by using a NdFeB permanent magnet, and the cell suspension was transferred into a 96 well plate (200 µl per well) and cultivated for 48 h. The control samples followed the same procedure.

Table 1
Concentration of MNPs used for cytotoxicity evaluation.

Sample composition[a]	MNPs concentration (mg/ml)
150 µl CM+50 µl SMN	2.50
180 µl CM+20 µl SMN	1.00
190 µl CM+10 µl SMN	0.50
195 µl CM+5 µl SMN	0.25

[a] CM stands for complete culture medium and SMN for suspension of magnetic nanoparticles.

The cytotoxicity of Fe–Cr–Nb–B MNPs was evaluated through the 5-dimethylthiazol-2-yl-2.5-diphenyltetrazolium bromide (MTT) assay by using DMSO as dissolution agent. The cell viability (%) of the samples was calculated using Eq. (1):

$$\text{Cell viability}\,(\%) = 100 \times \frac{OD_{FeCrNbB} - OD_{Blank}}{OD_{Control} - OD_{Blank}} \quad (1)$$

where OD represents the optical density of the wells containing: (a) cells and magnetic nanoparticles ($OD_{FeCrNbB}$), and (b) cells only ($OD_{Control}$). OD_{Blank} represents the optical density of the blank samples (cell culture medium without cells).

The absorbance of the samples was measured at 570 nm by using a plate reader (Triad LT-Dynex).

3. Results and discussions

Depending on body cross-section and tissue conductivity, AMFs with frequencies of around 100 kHz should be used for humans [15]. The applied frequency should be carefully chosen as it has been reported that frequencies lower than 50 kHz can lead to neuromuscular electro-stimulation, while frequencies higher than 10 MHz do not allow high penetration depth of the radiofrequency field, and, additionally, lead to the heating of tumor tissue's water [16]. The field frequency chosen in this experiment was under

200 kHz, therefore below electro-stimulation threshold and heating temperature range of the tissue water.

On the other hand, in order to be considered safe and tolerable for human body, the magnetic hyperthermia applications have to take into account a value of the product between the frequency and the intensity of the AMF $\leq 4.85 \times 10^8$ A m^{-1}s^{-1} [17]. However, this limiting value is imposed for the whole-body exposure, whereas for smaller body regions this critical value can be exceeded [8,18,19]. We used higher field parameters for our study, and, therefore, appropriate for smaller body regions.

3.1. Physical characterization of magnetic nanoparticles

The specific heating power of a magnetic material is linked to the weight concentration and magnetic properties, and conditioned by the limiting temperature used to affect cancerous cells. Generally, the recommended or tested concentrations for human-related magnetic hyperthermia are ranging from 5 to 30 mg/ml [20,21] or even more for clinical tests [22,23]. However, since for lower concentrations less biological side-effects are expected, a concentration up to 5 mg/ml of MNPs was considered to be adequate and effective enough for the hyperthermia tests.

For a ferromagnetic material, the heating efficiency is directly related to the hysteresis processes, the area of the hysteresis loop allowing the evaluation of the amount of heat generated per unit volume of magnetic material [24]. Fig. 4 shows the hysteresis loops of both chitosan-free and chitosan-coated $Fe_{68.2}Cr_{11.5}Nb_{0.3}B_{20}$ MNPs. The specific saturation magnetization of the coated-MNPs is lower as compared to chitosan-free MNPs due to the total weight of the sample, which includes the chitosan mass. However, while their remanent magnetization is similar, the coercive fields are slightly different (the inset of Fig. 4). Therefore, a lower power loss and, as consequence, a lower heating potential would be expected for chitosan-coated nanoparticles.

T_C controlled temperature in the 42–47 °C range is one of the most important parameters for *in-vivo* magnetic hyperthermia applications. Otherwise, if the temperature exceeds the critical limit, even if the damage rate of the cancerous cells can be consistently enhanced, the normal cells surrounding the tumor could be as well affected. For our low Curie temperature (T_C) materials, the power loss is severely reduced near Curie point compared with commonly used magnetite NPs, and, therefore, such materials are more suitable for self-regulating magnetic

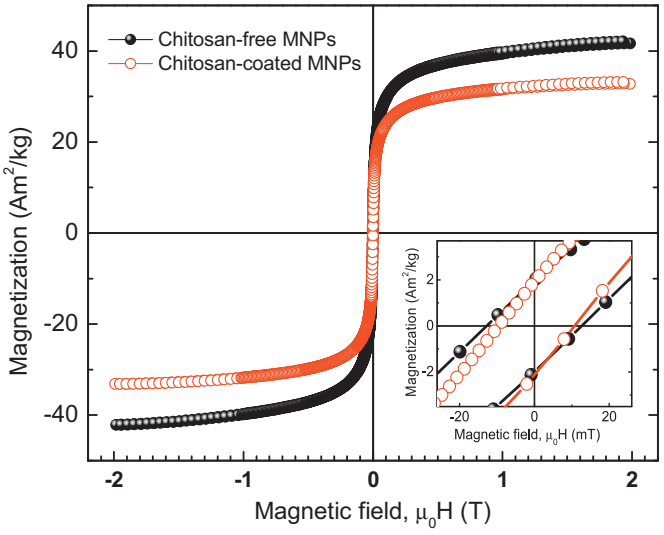

Fig. 4. Magnetization hysteresis loops of chitosan-coated MNPs (sample B) and chitosan-free MNPs (sample C). Inset: details from the near zero applied field.

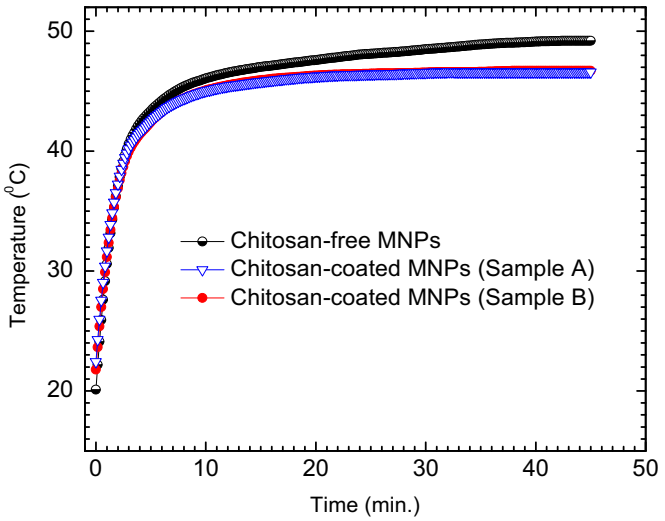

Fig. 5. The heating curves for the tested samples.

hyperthermia compared with Fe-oxide NPs. Our previous studies indicated a T_C near 50°C for $Fe_{67.7}Cr_{11.5}Nb_{0.3}B_{20}$ MNPs used in the present work [5].

Fig. 5 shows the heating curves for chitosan-free (Sample C) and chitosan-coated MNPs (Samples A and B). The heating curve of the chitosan-free glassy MNPs starts to saturate after 15 min. of continuous heating, when the temperature reaches 47 °C, and increases with only 2 °C during the next 25 min., when the equilibrium temperature is reached. This near constant temperature obtained for the chitosan-free glassy MNPs is about 2–3 °C higher than that of the chitosan-coated MNPs. However, the raise of the temperature induced by the coated-MNPs results into a 1 °C increase during the last 35 min. of continuous heating.

One should mention that AMF measurements of chitosan-free and chitosan-coated $Fe_{68.2}Cr_{11.5}Nb_{0.3}B_{20}$ MNPs for different applied magnetic fields always result in a steady-state temperature near T_C, independent of the magnetic field amplitude, only a change in the initial slope of the heating curve being observed. Such a specific behavior is a consequence of the fact that the energy generated by AMF must overcome the heat loss of the MNPs in suspension (the ascendant part of the heating curve), and is different compared with the heating behavior of Fe oxides MNPs with relatively high T_C ($>$ 550 °C) [2].

To quantitatively evaluate the heating efficiency of the powders, a caloric parameter such as the specific absorption rate (SAR)/specific loss power (SLP) can be calculated. The SAR (in W/g) represents the mass-normalized rate of energy absorption by a (biological) object and can be calculated by using the empirical formula [25]:

$$\mathrm{SAR} = (C/x)(dT/dt)_{t\to 0} \quad (2)$$

where C is the specific heat of the medium (generally, water) with magnetic material inside (generally equal to the specific heat of water, i.e. 4.185 J g^{-1} K^{-1}), dT/dt is the slope of the temperature *versus* time curve and x represents the ratio between the weight of the magnetic elements in the sample, in our case iron, and the weight of the liquid suspension.

SAR, calculated from the heating curves in the linear portion of the graph, varies rather narrowly (Table 2). The calculated SAR is in the range of the values obtained for ferrite-based magnetic nanofluids for slightly different field parameters [24,26]. However, as compared to the ferrofluids, starting from 44–46 °C the SAR of the Fe–Cr–Nb–B MNPs decreases towards zero, allowing to establish an equilibrium temperature in the sample.

Table 2
Specific absorption rates of the Fe–Cr–Nb–B MNPs coated (samples A and B) or not (sample C) with chitosan.

	Sample A	Sample B	Sample C
SAR (W/g)	189	192	215

3.2. Cytotoxicity evaluation

3.2.1. Simultaneous co-incubation

Fig. 6 shows the cell viability after 12 h of simultaneous co-incubation of cells in suspension with different concentrations of MNPs. As expected [27,28], the chitosan-coated MNPs (samples A and B) exhibit a pronounced tumoricidal effect, regardless of their concentration, with a tumoricidal peak for 2.5 mg/ml MNPs. For chitosan-free MNPs (sample C), the cell viability remains at high levels, except for the highest concentration of MNPs, when the viability is about 70%. There are also notable differences between chitosan-coated MNPs: for example, sample A turned out to be more efficient in inducing a significant tumoricidal effect, regardless of the MNPs concentrations, with a tumoricidal peak for the highest concentration.

The chitosan-free MNPs show good biocompatibility and a low tumoricidal outcome. When coated with chitosan, the toxicity of Fe–Cr–Nb–B MNPs increases against osteosarcoma cells in suspension, especially at high concentrations of MNPs, a similar behavior being observed previously for other types of particles coated with chitosan [28].

3.2.2. Delayed co-incubation

Fig. 7 shows the cell viability after 12 h of cells-MNPs co-incubation, when the MNPs addition was delayed for 6 h. The viability of the cells exposed to chitosan-coated MNPs is highly improved for all tested concentrations, as compared to the simultaneous co-incubation case presented in Section 3.2.1. On the other hand, the chitosan-free MNPs (sample C) induce a slight, but progressive, decrease in viability (the coefficient of variation, CV=0.0954) from 98% to about 80%, as the MNPs concentration increases, a behavior just slightly different compared with the simultaneous co-incubation results. However, in both cases (simultaneous co-incubation and delayed co-incubation, respectively), the chitosan-free MNPs exert the lowest decrease in cell viability, showing a good biocompatibility in a cell culture model.

For the delayed co-incubation approach, the major increase of the cell viability for chitosan-coated MNPs could be the result of the delayed cell-MNPs interaction that allows a partially-developed attachment of the cells to the plastic tube, affording them better survival conditions, as it can be presumed that cancerous

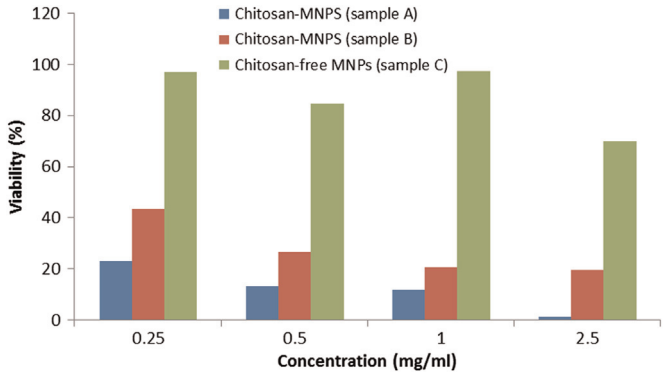

Fig. 6. Cell viability after 12 h of simultaneous co-incubation of cells in suspension with chitosan-free or chitosan-coated MNPs.

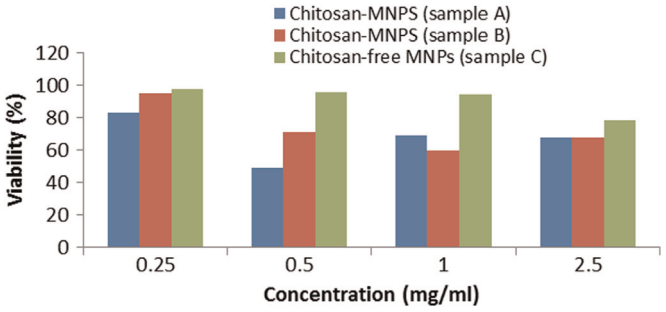

Fig. 7. Cell viability after 12 h of cell-MNPs co-incubation when the MNPs addition was delayed for 6 h.

cell network could have been developed at the moment when MNPs were introduced in the culture medium of the cells.

Depending on the MNPs concentration, the difference in the cell viability for each sample is considerably higher for the co-incubation approach as compared with the delayed co-incubation. Therefore, the MNPs concentration and incubation influence strongly the cell viability.

3.2.3. Cytotoxicity in AC magnetic fields

Following the 2 approaches presented above, the delayed co-incubation approach was considered for tests in AMF. The cell viability, before and after AMF-induced heating, was assessed by using the MTT assay, after magnetic separation of MNPs from the tubes and cell cultivation for 48 h. Fig. 8. shows the optical density (OD) values of all replicates. The cell viability, as calculated by Eq. (1), is 7.0% (sample A), 19.3% (sample B), 22.4% (samples C) in the presence of AMF and, respectively, 15.5% (sample A), 35.2% (sample B), and 58.1% (sample C) in the absence of AMF, as shown in Fig. 9. Each data point in Fig. 9, showing the cell viability after AMF exposure as compared with AMF-free conditions, was based on the OD values obtained from three wells. The statistical analysis, using *t*-test (two-sample assuming equal variances), has been performed in order to evaluate the statistical significance of the obtained results. The *p*-value ($p=0.0045$) pointed out a highly statistically significant viability decrease of the samples tested in AMF.

Therefore, all samples submitted to AMF-induced heating turned out to be highly efficient in developing tumor cell necrosis, decreasing to half the viability obtained by samples in AMF free-conditions. Our results are similar with the previous reports exploring the *in-vitro* antitumoral effect of MNPs in comparable conditions (adherent cancer cell lines treated with MNPs suspensions in magnetic field). The antitumoral activity of 50% and cell viability reduced up to 40.5% on B16-F10 melanoma cells was reported before for similar experiments [29].

It is presumable that the differences in cell viability obtained for samples tested in AMF-free conditions (Fig. 7) as compared with those tested in AMF-free conditions (Figs. 8 and 9), but used as control, emerged from the incubation conditions during the tests. Thus, for the results presented in Fig. 7 the tubes were incubated at 37 °C, 5% CO_2, 95% humidity, while in the latter tests (Figs. 8 and 9), the tubes were kept closed in a water bath, at 37 °C, fact that might influence the cell survival. Therefore, we consider that MNPs-mediated heating induces the decrease in the cell viability in this cell culture model, allowing a self-regulating magnetic hyperthermia by imposing an equilibrium temperature in high frequency AMF. The reported results are similar with current literature in terms of particle biocompatibility and efficiency of toxic effect on adherent cancer cell lines *in-vitro*. Our data add to a rather limited literature in the field, increasing the knowledge about MNPs behavior tested *in-vitro*, and allowing as well for taking the next step in the design of more complex

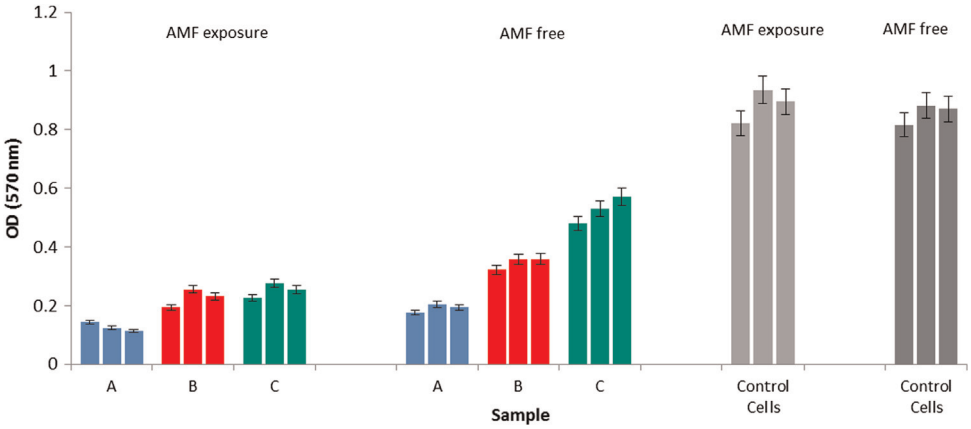

Fig. 8. Optical density (OD) at 570 nm of all triplicate samples after AMF exposure as compared with AMF-free conditions for 2.5 mg/ml concentration of MNPs. A and B represent chitosan-coated samples, while C stands for chitosan-free MNPs.

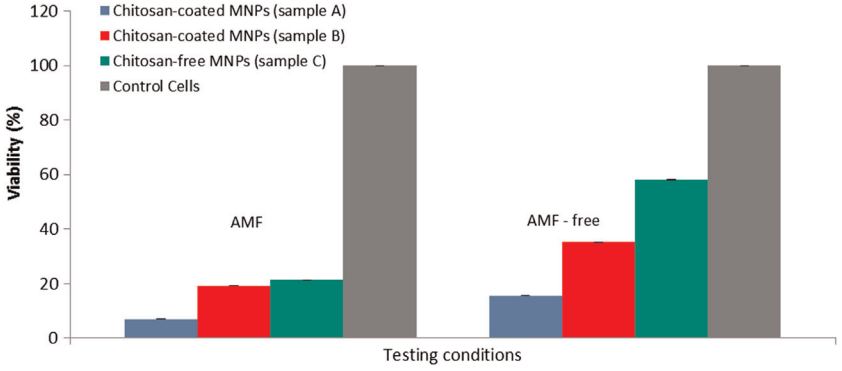

Fig. 9. Cell viability after AMF exposure as compared with AMF-free conditions for 2.5 mg/ml concentration of MNPs.

experimental conditions such as *in-vivo* experiments in animal models of tumor growth.

4. Conclusions

This work investigated the cytotoxicity of glassy $Fe_{68.2}Cr_{11.5}Nb_{0.3}B_{20}$ ferromagnetic nanoparticles, as such or coated with a chitosan layer, in the framework of a cell culture model. AMF measurements of chitosan-free and chitosan-coated $Fe_{68.2}Cr_{11.5}Nb_{0.3}B_{20}$ MNPs for different applied magnetic fields always result in a steady-state temperature near T_C, independent of the magnetic field amplitude. Chitosan-coated MNPs exhibit a pronounced cytotoxic effect in conditions of simultaneous MNPs-cellco-incubation. The cytotoxic effect changes, however, when the cells are allowed several hours to adapt to the new growing conditions, before MNPs co-incubation. On the other hand, the chitosan-free $Fe_{68.2}Cr_{11.5}Nb_{0.3}B_{20}$ MNPs show a good biocompatibility in the cancerous cell culture, regardless of the testing conditions. Most importantly, in high frequency alternating magnetic fields, the MNPs-mediated heating was proved to be a determining factor for cell viability decrease in the tested cell culture model. These results allow for further steps towards "*in vivo*" tests on animal model of tumor growth.

Acknowledgments

This work was supported by a CNDI-UEFISCDI Grant, Project no. 148/2012 (HYPERTHERMIA).

References

[1] F. Bray, A. Jemal, N. Grey, J. Ferlay, D. Forman, Global cancer transitions according to the human development index (2008–2030): a population-based study, Lancet Oncol. 13 (8) (2012) 790–801.
[2] Ch.S.S.R. Kumar, F. Mohammad, Magnetic nanomaterials for hyperthermia-based therapy and controlled drug delivery, Adv. Drug Deliv. Rev. 63 (2011) 789–808.
[3] A.E. Deatsch, B.A. Evans, Heating efficiency in magnetic nanoparticle hyperthermia, J. Magn. Magn. Mater. 354 (2014) 163–172.
[4] N. Lupu, H. Chiriac, S. Corodeanu, G. Ababei, Development of Fe–Nb–Cr–B glassy alloys with low Curie temperature and enhanced soft magnetic properties, IEEE Trans. Magn. 47 (10) (2011) 3791–3794.
[5] H. Chiriac, N. Lupu, M. Lostun, G. Ababei, M. Grigoras, C. Danceanu, Low TC Fe–Cr–Nb–B glassy submicron powders for hyperthermia applications, J. Appl. Phys. 115 (2014) 17B520.
[6] P.B. Shete, R.M. Patil, N.D. Thorat, A. Prasad, R.S. Ningthoujam, S.J. Ghosh, S. H. Pawar, Magnetic chitosan nanocomposite for hyperthermia therapy application: preparation, characterization and in vitro experiments, Appl. Surf. Sci. 288 (2014) 149–157.
[7] L.-F. Qi, Z.-R. Xu, Y. Li, X. Jiang, X.-Y. Han, In vitro effects of chitosan nanoparticles on proliferation of human gastric carcinoma cell line MGC803 cells, World J. Gastroenterol. 11 (33) (2005) 5136–5141.
[8] V. Zamora-Mora, M. Fernández-Gutiérrez, J. San Román, G. Goya, R. Hernández, C. Mijangos, Magnetic core–shell chitosan nanoparticles: rheological characterization and hyperthermia application, Carbohydr. Polym. 102 (2014) 691–698.
[9] H. Susanto, A.M. Samsudin, N. Rokhati, I.N. Widiasa, Immobilization of glucose oxidase on chitosan-based porous composite membranes and their potential use in biosensors, Enzyme Microb. Technol. 52 (6–7) (2013) 386–392.
[10] S. Rodrigues, M. Dionisio, C.R. Lopez, A. Grenha, Biocompatibility of chitosan carriers with application in drug delivery, J. Funct. Biomater. 3 (2012) 615–641.
[11] W. Gao, J.C.K. Lai, S.W. Leung, Functional enhancement of chitosan and nanoparticles in cell culture, tissue engineering, and pharmaceutical applications, Front. Physiol. 3 (321) (2012) 1–13.
[12] N.-L. Delgadillo-Armendariz, N.-A. Rangel-Vazquez, A.-I. García-Castanon, Spectroscopy analysis of chitosan–glibenclamide hydrogels, Spectrochim. Acta Part A: Mol. Biomol. Spectrosc. 120 (2014) 524–528.
[13] S.M.L. Silva, C.R.C. Braga, M.V.L. Fook, C.M.O. Raposo, L.H. Carvalho, E.L. Canedo, Application of infrared spectroscopy to analysis of chitosan/clay

nanocomposites, in: Theophile Theophanides (Ed.), Infrared Spectroscopy – Materials Science, Engineering and Technology, InTech, 2012, p. 51, ISBN:978-953-51-0537-4.
[14] R. Ramya, P.N. Sudha, Dr.J. Mahalakshmi, Preparation and characterization of chitosan binary blend, Int. J. Sci. Res. Publ. 2 (10) (2012) 1–9.
[15] A. Jordan, K. Maier-Hauff, P. Wust, M. Johannsen, Nanoparticles for thermotherapy, in: Ch. Kumar (Ed.), Nanomaterials for Cancer Therapy, Wiley-VCH Verlag GmbH & Co., Weinheim, 2006, p. 242, pp..
[16] E. Pollert, P. Veverka, M. Veverka, O. Kaman, K. Zaveta, S. Vasseur, R. Epherre, G. Goglio, E. Duguet, Search of new core materials for magnetic fluid hyperthermia: Preliminary chemical and physical issues, Prog. Solid State Chem. 37 (2009) 1–14.
[17] G.F. Goya, E. Lima, A.D. Arelaro, T. Torres, H.R. Rechenberg, L. Rossi, C. Marquina, M.R. Ibarra, Magnetic hyperthermia with FeO nanoparticles: the influence of particle size on energy absorption, IEEE Trans. Magn. 44 (11) (2008) 4444–4447.
[18] R. Hergt, S. Dutz, Magnetic particle hyperthermia-biophysical limitations of a visionary tumour therapy, J. Magn. Magn. Mater. 311 (2007) 187–192.
[19] D.S. Nikam, S.V. Jadhav, V.M. Khot, M.R. Phadatare, S.H. Pawar, Study of AC magnetic heating characteristics of $Co_{0.5}Zn_{0.5}Fe_2O_4$ nanoparticles for magnetic hyperthermia therapy, J. Magn. Magn. Mater. 349 (2014) 208–213.
[20] J. Qu, G. Liu, Y. Wang, R. Hong, Preparation of Fe_3O_4–chitosan nanoparticles used for hyperthermia, Adv. Powder Technol. 21 (2010) 461–467.
[21] D.-H. Kim, D.E. Nikles, D.T. Johnson, C.S. Brazel, Heat generation of aqueously dispersed $CoFe_2O_4$ nanoparticles as heating agents for magnetically activated drug delivery and hyperthermia, J. Magn. Magn. Mater. 320 (2008) 2390–2396.
[22] M. Johannsen, U. Gneveckow, L. Eckelt, A. Feussner, N. Waldofner, R. Scholz, S. Deger, P. Wust, S.A. Loening, A. Jordan, Clinical hyperthermia of prostate cancer using magnetic nanoparticles: presentation of a new interstitial technique, Int. J. Hyperth. 21 (7) (2005) 637–647.
[23] M. Johannsen, B. Thiesen, P. Wust, A. Jordan, Magnetic nanoparticle hyperthermia for prostate cancer, Int. J. Hyperth. 26 (8) (2010) 790–795.
[24] R. Hergt, S. Dutz, R. Müller, M. Zeisberger, Magnetic particle hyperthermia: nanoparticle magnetism and materials development for cancer therapy, J. Phys.: Condens. Matter 18 (2006) S2919–S2934.
[25] Y. Krupskaya, C. Mahn, A. Parameswaran, A. Taylor, K. Kramer, S. Hampel, A. Leonhardt, M. Ritschel, B. Büchner, R. Klingeler, Magnetic study of iron-containing carbon nanotubes: feasibility for magnetic hyperthermia, J. Magn. Magn. Mater. 321 (2009) 4067–4071.
[26] Sharifi, H. Shokrollahi, S. Amiri, Ferrite-based magnetic nanofluids used in hyperthermia applications, J. Magn. Magn. Mater. 324 (2012) 903–915.
[27] L. Qi, Z. Xu, X. Jiang, Y. Li, M. Wang, Cytotoxic activities of chitosan nanoparticles and copper-loaded nanoparticles, Bioorg. Med. Chem. Lett. 15 (2005) 1397–1399.
[28] M. Hasegawa, K. Yagi, S. Iwakawa, M. Hirai, Chitosan induces apoptosis via Caspase-3 activation in bladder tumor cells, Jpn. J. Cancer Res. 92 (2001) 459–466.
[29] A.M. Falqueiro, M.P. Siqueira-Moura, D.R. Jardim, F.L. Primo, P.C. Morais, E. Mosiniewicz-Szablewska, P. Suchocki, A.C. Tedesco, *In vitro* cytotoxicity of Selol-loaded magnetic nanocapsules against neoplastic cell lines under AC magnetic field activation, J. Appl. Phys. 111 (7) (2012) 07B335.